

# Analysis of Cylinder Block Torque Characteristics of Dual-Drive Axial Piston Motor

**Haishun DENG, Wenjun CHAI, Cong HU**

*School of Mechanical Engineering, Anhui University of Science and Technology, Huainan, Anhui 232001, PR China,  
E-mail: dhs1998@163.com*

**crossref** <http://dx.doi.org/10.5755/j02.mech.28730>

## 1. Introduction

The torque characteristics of axial piston motors are a mechanical representation of the external load and the internal structure (swashplate, distributor, piston), which directly reflects the overall performance of the axial piston motor. The cylinder block of the press motor is always subject to a pulsating torque, part of which is the motor's driving torque, the pulsation rate of which reflects the stability of the motor's operation. In order to reduce the pulsation rate of the motor output torque, reduce the overturning moment of the cylinder block, and ensure the stability of the hydraulic motor operation, domestic and foreign scholars take many methods [1]. Desen Wen et al. designed a multi-slant disk multi-emission motor. Studies have shown that when the inner and external motors are fully operational, the torque unevenness factor is effectively reduced and an experimental platform was built to verify the theoretical correctness by deriving several sets of experimental data through the JN338 torque measuring instrument, and the results were approximated to the numerical analysis [2]. Songlin Nie derived the torque equation for a piston motor with closed dead space, and the analysis shows that the torque pulsation rate is affected by the number of plugs and the closed dead space [3]. The other part of the cylinder block is expressed as the overturning moment of the cylinder block, the moment makes the cylinder block's position tilted, so that the mating vice form wedge-shaped oil film, and even make the mating vice bias wear and cause oil leakage [4, 5]. Wiczorek et al. in Germany developed the simulation tool CASPAR independently and simulated and analyzed the axial piston pump lubrication gap flow, and the study found that the asymmetrically distributed moment to which the cylinder block was subjected caused it to overturn [6]. Based on the wedge-shaped oil film theory, Hu et al. solved the dynamic pressure of the distribution sub oil film and found that the rotor was subjected to the superposition of two eccentric distances, which caused the distribution sub oil film to vary periodically [7]. Zhaoqiang Wang et al. used the finite difference method to solve the oil film equation for the flow distribution subdivision, and the results showed that the cylinder block of the common piston pump tilted due to the different oil pressure on both sides, which in turn caused the burned disk [8]. Shuze Li et al. investigated the relationship between the pulsation characteristics of the hydraulic moment of the flow distribution disc on the cylinder block and the closing angle, taking into account the process of gradual pressure change in the piston pump cylinder block and the stability of the oil pressure field between the flow distribution disc and the rotor on the cylinder block acting moment was investigated [9]. Scholars have made

some studies to reduce the effect of cylinder block overturning moment [10, 11]. Ivantysyn et al. proposed to add additional bearings to the external ring of the cylinder block to counteract the overturning moment and to increase the stiffness of the rotating shaft to reduce its deflection deformation to ensure that the cylinder block does not tilt [12]. Haishun Deng et al. showed that weaving can effectively reduce the friction coefficient and the frictional wear of the mating substrate through experiments.

Double-sided drive axial piston motor cylinder block is subject to high pressure hydraulic pressure on both sides, which is well balanced and has better mechanical characteristics than ordinary piston motors [13]. However, the research is not deep, and its potential for improvement and optimization is large. Haishun Deng et al. analyzed the influence of the structural parameters of the dual-drive motor on the friction torque and analyzed the basic characteristics of the starting speed and torque [14]. Due to the special structure of the double-sided drive axial piston motor, the force situation of its cylinder block body is different from that of ordinary axial piston motor. For this reason, it is necessary to conduct a detailed analysis of the torque on the motor block, in order to provide some reference for the design and manufacture of the dual side drive axial piston motor block.

## 2. Mathematical model of cylinder block torque of dual-drive axial piston motor

The total torque of the double-sided drive axial piston motor cylinder block is mainly generated by the combined effect of the torque generated by the piston - slide shoe assembly, the cylinder block friction torque loss, and the counter-thrust torque of the oil film of the flow distribution sub. In order to better study the total torque of the cylinder block, the mathematical model of each torque and the total torque of the cylinder block of the dual side drive axial piston motor was firstly established, and then the influence of each factor on the cylinder block torque was analyzed.

### 2.1. Torque generated by the plunger-slide shoe assembly

Double-sided drive axial piston motor plunger-slide shoe assembly rotates with the cylinder block at high-speed circular rotation while performing reciprocating linear motion in the cylinder block bore. As shown in Fig.1. Take the intersection of the spindle axis and the contact surface of the flow distribution subsystem as the coordinate origin  $o$ . The  $z$ -axis points to the swashplate along the axis, the  $y$ -axis is perpendicular to the spindle axis and points to the lower dead point of the external emission of pistons. De-

termine the  $x$ -axis according to the right-hand rule. To create the coordinate system  $o-xyz$ . Initial state with the center of the inner plunger ball head in the upper dead center position. After the inner and external pistons have turned clockwise with the cylinder block for time  $t$ . The expression for the angle of rotation of the center of an arbitrary inner and external emission of plunger ball hinges at any moment is:

$$\varphi_{eu} = \omega t + (u-1) \frac{2\pi}{n_e} + \gamma \operatorname{sgn}(e-1), \quad (1)$$

where:  $e$  is markings of emission; where  $e=1$  means internal emission and  $e=2$  means external emission;  $\varphi_{eu}$  is inner emission; external emission  $u$ th plunger spindle angle, °;  $n_e$  is number of internal and external pistons;  $\omega$  is spindle speed, °/s;  $\gamma$  is staggered angle of the inner and external plunger emissions, °;  $t$  is spindle rotation time, s.

If the plunger motion is expressed in terms of the coordinates of the center of the ball hinge of the inner and external emissions of any plunger. Be expressed as:

$$\left. \begin{aligned} x_{eu} &= r_e \sin \varphi_{eu} \\ y_{eu} &= r_e \cos \varphi_{eu} \\ z_{eu} &= l_0 - r_e \tan \beta_e \cos \varphi_{eu} \operatorname{sgn}(e-1.5) \end{aligned} \right\}, \quad (2)$$

where:  $r_e$  is radius of the center distribution circle of the inner and external emission of plunger ball hinges, mm;  $\beta_e$  is tilt angle of inner and external swashplate, °;  $l_0$  is distance from the origin  $o$  to the intersection  $H$  of the line connecting the center of the inner and external emission of plunger hinges in the  $o-xy$  plane (mm).

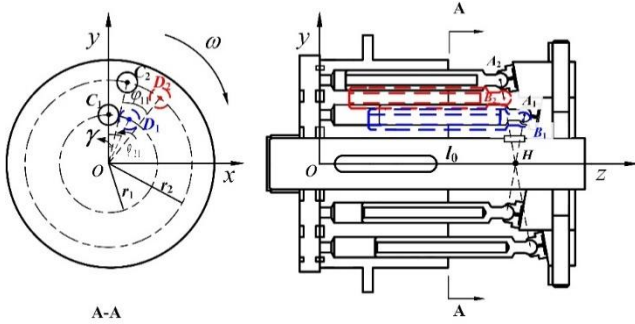


Fig. 1 Plunger movement diagram for dual-drive axial piston motor

The derivative of Eq. (2) gives the expression for the velocity vector at the center of the plunger ball hinge as:

$$\begin{aligned} \mathbf{v}_{eu} &= \omega r_e (\cos \varphi_{eu} \mathbf{i} - \sin \varphi_{eu} \mathbf{j}) + \\ &+ \omega r_e \tan \beta_e \sin \varphi_{eu} \operatorname{sgn}(e-1.5) \mathbf{k}. \end{aligned} \quad (3)$$

Further derivation of Eq. (3) yields an expression for the acceleration vector at the center of the inner and external plunger ball hinges as:

$$\begin{aligned} \mathbf{a}_{eu} &= -\omega^2 r_e (\sin \varphi_{eu} \mathbf{i} + \cos \varphi_{eu} \mathbf{j}) + \\ &+ \omega^2 r_e \tan \beta_e \cos \varphi_{eu} \operatorname{sgn}(e-1.5) \mathbf{k}. \end{aligned} \quad (4)$$

where:  $v_{eu}$  is velocity of the center of the  $u$ th plunger ball head in the inner and external emissions, m/s;  $a_{eu}$  acceleration of the center of the  $u$ th plunger ball head in the inner

and external emissions, m/s<sup>2</sup>;  $\mathbf{i}$ ,  $\mathbf{j}$  and  $\mathbf{k}$  were spatial coordinate vector.

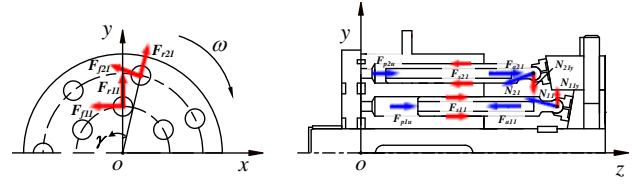


Fig. 2 Force diagram of the plunger-slide shoe assembly

The forces on the plunger-slide shoe assembly of a double-sided driven axial plunger motor are shown in Figs. 2 and 3. Centrifugal forces, reciprocating inertia forces, plunger frictional forces and plunger-slide shoe frictional forces will be generated by the plunger-slide shoe assembly in the inner and external emissions. And acts on the cylinder block by means of an oil film. This produces a tipping torque on the cylinder block and a driving torque to turn the cylinder block.

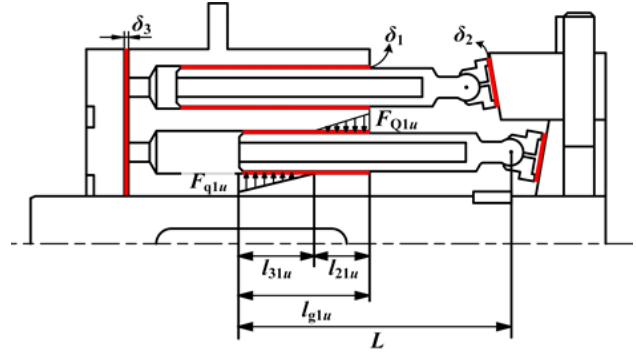


Fig. 3 Plunger to cylinder block bore force

From the above it follows that the vector expressions for the position of the center of mass and the center of the ball hinge of the inner and external emission plunger-slide shoe assembly are as follows:

$$\begin{aligned} \mathbf{l}_{zeu} &= r_e \sin \varphi_{eu} \mathbf{i} + r_e \cos \varphi_{eu} \mathbf{j} + \\ &+ [l_0 - r_e \tan \beta_e \cos \varphi_{eu} \operatorname{sgn}(e-1.5) - l_s] \mathbf{k}, \end{aligned} \quad (5)$$

$$\begin{aligned} \mathbf{l}_{reu} &= r_e \sin \varphi_{eu} \mathbf{i} + r_e \cos \varphi_{eu} \mathbf{j} + \\ &+ [l_0 - r_e \tan \beta_e \cos \varphi_{eu} \operatorname{sgn}(e-1.5)] \mathbf{k}, \end{aligned} \quad (6)$$

where;  $l_{reu}$  and  $l_{zeu}$  is center of mass and ball hinge position of the  $u$ th plunger-slide shoe assembly in the inner and external emissions;  $l_s$  distance between the center of mass of the plunger-slide shoe assembly and the center of the ball hinge, mm.

From the expressions for the acceleration vector at the center of the inner and external plunger ball-heads we get the centrifugal forces  $F_{reu}$  and reciprocating inertia forces  $F_{aeu}$  for an arbitrary plunger-slip shoe assembly are:

$$\mathbf{F}_{reu} = m_1 \omega^2 r_e (\sin \varphi_{eu} \mathbf{i} + \cos \varphi_{eu} \mathbf{j}) + 0 \mathbf{k}, \quad (7)$$

$$\mathbf{F}_{aeu} = 0 \mathbf{i} + 0 \mathbf{j} + m_1 \omega^2 r_e \tan \beta_e \cos \varphi_{eu} \operatorname{sgn}(e-1.5) \mathbf{k}. \quad (8)$$

When the slide shoe rotates on the swashplate, the swashplate exerts a frictional force on the slide shoe, approximating this frictional force to the center of the ball

hinge. Double side drive axial piston motor with hydrostatically supported slide shoe construction. Ignoring the spin and tipping of the skid shoe. Relative motion of the slide shoe to the swashplate under purely liquid friction conditions. The viscous friction  $F_{feu}$  of the sliding shoe sub is obtained as:

$$F_{feu} = \mu_0 \omega \pi \frac{r_e}{\delta_2} (R_G^2 - r_G^2) (-\cos\varphi_{eu} \mathbf{i} + \sin\varphi_{eu} \mathbf{j}), \quad (9)$$

where:  $\delta_2$  is sliding shoe sub oil-film thickness,  $\mu\text{m}$ ;  $\mu_0$  is dynamic viscosity of oil at standard atmospheric pressure,  $\text{pa}\cdot\text{s}$ ;  $R_G$  is sliding shoe oil sump external diameter,  $\text{mm}$ ;  $r_G$  is sliding shoe oil sump inner diameter,  $\text{mm}$ .

In order to ensure that the slide shoe is always tight against the swashplate during normal motor operation. A pre-compressed center spring provides compression for the slide shoe via a return ball hinge. Assume that the spring force on each plunger shoe assembly is of uniform magnitude. Then the spring force can be expressed as:

$$F_{the} = \frac{F_{te}}{n_e}, \quad (10)$$

where:  $F_{the}$  is spring forces on individual pistons for internal and external discharge;  $F_{te}$  is total spring force provided by the inner and external emission of pre-compression springs.

The high-speed reciprocating motion of the plunger-slip shoe assembly generates axial forces (reciprocating inertia forces, plunger cavity oil forces and plunger sub friction) that will cause the swashplate to generate support forces  $N_{eu}$  on the slip shoe. The division of this support force along the y-axis produces a tilting moment  $N_{yeu}$  and a driving torque on the cylinder block through the center of the ball hinge. This converts hydraulic energy into mechanical energy. Refer to Figs. 3 and 4, if the forces on the plunger-slide shoe assembly are balanced we get the following:

$$N_{eu} \sin\beta_e = F_{Qeu} - F_{qeu}, \quad (11)$$

$$N_{eu} \cos\beta_e = F_{deu} + F_{aeu} + F_{seu} + F_{the}, \quad (12)$$

$$F_{Qeu} \left( L - l_{1eu} + \frac{l_{2eu}}{3} \right) - F_{qeu} \left( L - \frac{l_{3eu}}{3} \right) - (fF_{Qeu} r_3 - fF_{qeu} r) \operatorname{sgn}((e-1.5)(-\sin(a))) = 0, \quad (13)$$

$$l_{g2u} = 44 - r_2 \tan\beta_2 (1 - \cos\varphi_{2u}), \quad (14)$$

$$l_{g1u} = (44 - 2r_1 \tan\beta_1) + r_1 \tan\beta_1 (1 - \cos\varphi_{1u}), \quad (15)$$

$$l_{geu} = l_{2eu} + l_{3eu} = l_2 \operatorname{sgn}(e-1) - l_1 \operatorname{sgn}(e-2) + r_e \tan\beta_e \cos\varphi_{eu} \operatorname{sgn}(e-1.5). \quad (16)$$

From the force analysis shown in Fig. 4, and further based on the principle of similarity of force distribution triangles, we get:

$$\frac{F_{Qeu}}{F_{qeu}} = \frac{l_{2eu}^2}{l_{3eu}^2}, \quad (17)$$

where:  $F_{Qeu}$  and  $F_{qeu}$  is lateral pressure of the cylinder block bore on the plunger,  $\text{N}$ ;  $F_{deu}$  is plunger chamber oil force,  $\text{N}$ ;

$F_{aeu}$  is reciprocating inertia forces in the plunger-slide shoe assembly,  $\text{N}$ ;  $F_{seu}$  is plunger sub friction,  $\text{N}$ ;  $L$  is plunger length,  $\text{mm}$ ;  $f$  is friction coefficient of the plunger sub, and  $l_{gue}$  is internal and external plunger retention cylinder block length,  $\text{mm}$ ;  $r_3$  is plunger radius,  $\text{mm}$ .

For the plunger-slide shoe assembly, the direction of frictional force on the plunger subassembly is always opposite to the speed of the plunger movement. However, the cylinder block is subjected to frictional forces in the same direction as the velocity of the plunger movement. Solving for:

$$F_{seu} = (F_{Qeu} + F_{qeu}) f \operatorname{sgn}((e-1.5)(-\sin(a))). \quad (18)$$

The expression for the oil force  $F_{deu}$  in the plunger chamber is as follows:

$$F_{deu} = p_{eu} \pi r_3^2, \quad (19)$$

where:  $p_{eu}$  is Plunger chamber oil pressure,  $\text{MPa}$ .

The dynamic changes in oil pressure during suction and discharge in each plunger chamber at different angles of rotation are taken into account in the calculation process. Using the plunger chamber as a control body. The oil in the plunger chamber is a compressible fluid. The equation for the dynamic pressure characteristics of the fluid is obtained as follows:

$$\frac{dp_{eu}}{dt} = \frac{E}{\pi r_3^2 (l_g - l_{geu})} (Q_{in} - Q_{out} - Q_{hl} - Q_{zl} - Q_{pl} - Q_v), \quad (20)$$

where:  $l_g$  is cylinder block bore length,  $\text{mm}$ ;  $l_{geu}$  is plunger retention length,  $\text{mm}$ ;  $Q_{in}$  is plunger chamber oil suction volume,  $\text{m}^3/\text{s}$ ;  $Q_{out}$  is plunger chamber oil discharge,  $\text{m}^3/\text{s}$ ;  $Q_{hl}$  is sliding shoe sub-leakage,  $\text{m}^3/\text{s}$ ;  $Q_{z1}$  is plunger sub-leakage,  $\text{m}^3/\text{s}$ ;  $Q_{p1}$  is distribution sub-leakage,  $\text{m}^3/\text{s}$ .

$$Q_v = \pi \omega r_e r_3^2 \tan\beta_e \sin\varphi_{eu} \operatorname{sgn}(e-1.5). \quad (21)$$

Assuming laminar flow between the friction sub-assemblies and without considering the dynamic characteristics of leakage. The expression for the leakage flow due to shear and differential pressure for a single plunger pair is as follows:

$$Q_{zl} = \frac{r_3 \pi \delta_1^3 (p_{ine} - p_{out})}{6 \mu_0 l_{geu}} + r_3 \pi \delta_1 v_{eu}, \quad (22)$$

where:  $\delta_1$  is plunger sub unilateral clearance,  $\mu\text{m}$ ;  $p_{ine}$  is oil-suction pressure of internal and external plunger,  $\text{MPa}$ ;  $p_{out}$  is oil-emission pressure,  $\text{MPa}$ .

The leakage flow rate of a single slip shoe sub is:

$$Q_{hl} = \frac{\pi \delta_2^3 (p_{ine} - p_{out})}{6 \mu_0 (R_G / r_G)}. \quad (23)$$

The dual side drive axial piston motor has a flat flow distribution disc. Its distribution sub-leakage flow is:

$$Q_{pl} = \frac{\pi \delta_3^3 (\pi \alpha_e / 180) (p_{ine} - p_{out})}{12 \mu_0} \times \left[ \frac{1}{\ln(r_{e5} / r_{e4})} + \frac{1}{\ln(r_{e7} / r_{e6})} \right], \quad (24)$$

where:  $\alpha_e$  is internal and external distribution discs with waist-shaped slotted corners, °;  $\delta_3$  is flow distribution sub clearance,  $\mu\text{m}$ ;  $r_{e4}$  and  $r_{e6}$  are external diameter of internal and external sealing tape, mm;  $r_{e5}$  and  $r_{e7}$  are inner diameter of internal and external sealing tape, mm.

$$\left. \begin{aligned} Q_{in} &= C_d A_{in} \sqrt{\frac{2(p_{me} - p_{eu})}{\rho}} \\ Q_{out} &= C_d A_{out} \sqrt{\frac{2(p_{eu} - p_{out})}{\rho}} \end{aligned} \right\}, \quad (25)$$

where:  $C_d$  is flow distribution sub-throttling coefficient;  $A_{in}$  is overflow area between cylinder waist hole and inlet-drainage port of flow distribution Plate,  $\text{mm}^2$ ;  $A_{out}$  is overflow area between cylinder waist hole and oil-drainage port of flow distribution Plate,  $\text{mm}^2$ ;  $\rho$  is oil density,  $\text{kg/m}^3$ .

## 2. 2. Cylinder block friction torque loss

The friction torque loss of each friction pair during the operation of a double-sided drive axial piston motor has a certain influence on the motor output torque. Its main frictional torque losses can be divided into the following three

$$\begin{aligned} T_z &= \int_{r_{14}}^{r_{15}} \int_{\varphi_{11}}^{\varphi_{12}} \left( 1 + 0.003 \frac{\ln r - \ln r_{14}}{\ln r_{15} - \ln r_{14}} p_s \right) \mu_0 \omega r^2 / hd \varphi dr + \int_{r_{16}}^{r_{17}} \int_{\varphi_{13}}^{\varphi_{14}} \left( 1 + 0.003 \frac{\ln r_{17} - \ln r}{\ln r_{17} - \ln r_{16}} p_s \right) \mu_0 \omega r^2 / hd \varphi dr + \\ &+ \int_{r_{14}}^{r_{15}} \int_{\varphi_{13}}^{\varphi_{14}} \left( 1 + 0.003 \frac{\ln r_{17} - \ln r}{\ln r_{17} - \ln r_{16}} p_0 \right) \mu_0 \omega r^2 / hd \varphi dr + \int_{r_3}^{r_4} \int_{\varphi_{11}}^{\varphi_{12}} \left( 1 + 0.003 \frac{\ln r - \ln r_{14}}{\ln r_{15} - \ln r_{14}} p_0 \right) \mu_0 \omega r^2 / hd \varphi dr + \\ &+ \int_{r_{17}}^{r_{24}} \int_0^{2\pi} \left( 1 + 0.003 p_s \right) \mu_0 \omega r^2 / hd \varphi dr + \int_{r_{24}}^{r_{25}} \int_{\varphi_{21}}^{\varphi_{22}} \left( 1 + 0.003 \frac{\ln r - \ln r_{24}}{\ln r_{25} - \ln r_{24}} p_s \right) \mu_0 \omega r^2 / hd \varphi dr + \\ &+ \int_{r_{26}}^{r_{27}} \int_{\varphi_{23}}^{\varphi_{24}} \left( 1 + 0.003 \frac{\ln r_{27} - \ln r}{\ln r_{27} - \ln r_{26}} p_s \right) \mu_0 \omega r^2 / hd \varphi dr + \int_{r_{24}}^{r_{25}} \int_{\varphi_{21}}^{\varphi_{22}} \left( 1 + 0.003 \frac{\ln r - \ln r_{24}}{\ln r_{25} - \ln r_{24}} p_0 \right) \mu_0 \omega r^2 / hd \varphi dr + \\ &+ \int_{r_{26}}^{r_{27}} \int_{\varphi_{23}}^{\varphi_{24}} \left( 1 + 0.003 \frac{\ln r_{27} - \ln r}{\ln r_{27} - \ln r_{26}} p_0 \right) \mu_0 \omega r^2 / hd \varphi dr + \int_{r_{14}}^{r_{17}} \left[ 2 \int_{\varphi_{15}}^{\varphi_{16}} \left( 1 + 0.003 \frac{p_0 + p_s}{2} \right) \mu_0 \omega r^2 / hd \varphi \right] dr + \\ &+ \int_{r_{24}}^{r_{27}} \left[ 2 \int_{\varphi_{25}}^{\varphi_{26}} \left( 1 + 0.003 \frac{p_0 + p_s}{2} \right) \mu_0 \omega r^2 / hd \varphi \right] dr. \end{aligned} \quad (27)$$

### 2) Frictional torque at bearings.

From the construction of a double side drive axial piston motor: The rotating shaft is mainly supported by two bearings. The radial component of the support force of the swashplate on the slide shoe is applied to the rotation shaft via the cylinder block. As a result, a corresponding support reaction force is generated at the bearing and a frictional torque is generated opposite to the driving torque.

The radial load acting on the shaft through the cylinder block by the swashplate support reaction is:

$$F_b = \sum_{u=1}^{n_1} N_{1u} \sin \beta_1 + \sum_{u=1}^{n_2} N_{2u} \sin \beta_2. \quad (28)$$

The magnitude of the support reaction force generated by this radial load on the two bearings is:

$$F_{b1} = \frac{l_{z1}}{l_{z1} + l_{z2}} F_b, \quad (29)$$

categories: 1) Frictional torque of the flow distribution sub; 2) Frictional torque at bearings; 3) Sliding shoe sub friction torque.

### 1) Frictional torque of the flow distribution sub.

The structure of the flow distribution subsystem of the double-sided drive axial piston motor is more complex. It is necessary to divide its flow distribution sub oil film into several areas in detail. The pressure distribution in each region is then found. The total frictional torque is obtained by summing up the frictional torque of each area according to Newton's viscosity law. Assuming full oil film lubrication and negligible oil film thickness variation in the flow distribution substrate. Then the frictional torque of the flow distribution sub after taking into account the viscous pressure characteristics of the oil is:

$$T = \int_{r_1}^{r_2} \int_{\varphi_1}^{\varphi_2} \left[ (1 + 0.003 p) \mu_0 \omega r^2 / \delta_3 \right] d\varphi dr, \quad (26)$$

where:  $r$  is circle radius, mm;  $\varphi$  is rounded corners, °.

The total frictional torque  $T_z$  of the distribution sub-oil film can be obtained according to the division of the region in reference as [15]:

$$F_{b2} = \frac{l_{z2}}{l_{z1} + l_{z2}} F_b, \quad (30)$$

where:  $l_{z1}$  and  $l_{z2}$  are distance from the bearing support point at the front and rear ends to the point of action of the radial component force, mm.

Eqs. (29 – 31) further yield the magnitude of the frictional torque of the bearings at both ends as:

$$T_b = f_b F_{b1} r_{b1} + f_b F_{b2} r_{b2}, \quad (31)$$

where:  $f_b$  is bearing friction coefficient;  $r_{b1}$ ,  $r_{b2}$  are radius of front and rear end bearings, mm.

## 2.3. Counter-thrust torque of the flow distribution sub-film

When the high pressure oil in the plunger chamber flows into the gap between the flow distribution disc and the cylinder block and is in radial laminar flow. The counter-

thrust will be generated by the formation of the flow distribution sub-film. This counter-thrust tends to push the cylinder block away from the flow distribution plate. Due to the nature of the piston motor, the pressure field in the suction and discharge zones is different, resulting in the cylinder block always being subjected to an overturning moment that tilts its stance. For the dual drive axial piston motor. In the

case of double-sided drive axial piston motors, there are high and low pressure areas on both sides of the distributor, which allows the counter-thrust torque to be offset to some extent.

The counter thrust moment of the flow distribution sub oil film is [16]:

$$T_{ft} = \sum_{e=1}^2 \frac{2p_{ine}}{9} \left[ \frac{r_{e7}^3 - r_{e6}^3}{\ln(r_{e7}/r_{e6})} - \frac{r_{e5}^3 - r_{e4}^3}{\ln(r_{e5}/r_{e4})} \right] \cos \frac{\psi_e - \alpha_e}{2} \cos \frac{\psi_e}{4} \text{sgn}(e-1.5), \quad (32)$$

where:  $\psi_e$  is angular spacing between inner and external plunger emissions, °;  $\alpha_e$  is internal and external distribution discs with waist-shaped slotted corners, °.

#### 2.4. Total cylinder block torque

From the above analysis it follows that: moments

$$M_z = \sum_{e=1}^2 \sum_{u=1}^{n_e} (F_{reu} \times l_{zeu} + F_{feu} \times l_{reu} - F_{seu} \times l_{reu} + N_{eu} \times l_{reu}) + T_{ft} \cdot j - (T_z + T_b) \cdot k. \quad (33)$$

Torque pulsation rates of:

$$\varepsilon = \left| \frac{T_{max} - T_{min}}{T_p} \right| \times 100\%. \quad (34)$$

### 3. Results and analysis

Dual side drive axial piston motors can be considered as a superposition of two single emission piston motors. It is important to consider not only the influence of key parameters such as the number of plugs, suction pressure and swashplate inclination on the overturning torque and

around the  $x$ ,  $y$  and  $z$  axes for a bilaterally driven axial piston motor cylinder block. Where the moments around the  $x$  and  $y$  axes are the tipping moments that cause the cylinder block position to tip over. The torque around the  $z$ -axis is the output torque of the piston motor. With a positive clockwise moment around each axis. Then the expression for the total torque generated on the cylinder block is as follows:

output torque of a common single-emission axial piston pump, but also the influence of the staggering angle on its torque characteristics. The phase difference between the torque applied to the inner and external emissions is determined by the characteristic staggering angle of the double-sided drive axial piston motor. This affects the magnitude of the total torque and the pulsation rate. In summary, the main factors affecting the individual moments applied to the cylinder block of a double-sided drive axial piston motor include: Number of pistons, staggering angle, oil inlet pressure and swashplate inclination. The torque pulsation rate of the twin drive motor block will be analyzed using the above four parameters as variables. Other basic calculation parameters are shown in Table 1.

Table 1

Main calculation parameters

| Symbols and units           | Physical significance   | Numerical values | Symbols and units        | Physical significance  | Numerical values |
|-----------------------------|---|------------------|--------------------------|--|------------------|
| $\rho$ , kg/m <sup>3</sup>  | Oil density   | 850              | $p_{ine}$ , MPa          | Oil inlet pressure   | 31.5             |
| $E$ , MPa                   | Oil bulk modulus  | 700              | $p_{out}$ , MP)          | Oil return pressure  | 0.1              |
| $\delta_1$ /()              | Plunger sub unilateral clearance  | 6                | $r_{14}$ , $r_{24}$ , mm | Inner and external emission internal sealing tape inner diameter | 18, 36           |
| $\delta_2$ , $\mu\text{m}$  | Sliding shoe sub clearance  | 5                | $r_{17}$ , $r_{27}$ , mm | Internal and external sealing tape diameter                      | 30, 46           |
| $\delta_3$ , $\mu\text{m}$  | Flow distribution sub clearance   | 6                | $R_G$ , $r_G$ mm         | Sliding shoe oil sump external and inner diameter                | 8, 5             |
| $\alpha_1$ , $\alpha_2$ , ° | Internal and external flow distribution discs with waist-shaped grooves wrapping the corner | 153.9, 147       | $l_g$ , mm               | Cylinder block bore length                                       | 55               |
| $\mu_0$ , pa0s              | Standard atmospheric pressure fluid dynamic viscosity                                       | 0.02             | $C_d$                    | Throttling factor  | 0.7              |
| $r_3$ , mm                  | Plunger radius  | 5                | $\omega/r$ , min         | Rotational speed   | 1500             |
| $F_{sz}$ , N                | Spring force  | 450              | $r_1$ , $r_2$ , mm       | Radius of distribution circle                                    | 24, 41           |

#### 3.1. Effect of plunger number on cylinder block torque

Fig. 4 shows the effect of the number of plugs on the torque applied to the cylinder block of a double-sided driven axial piston motor. As can be seen from Fig. 4 during one working cycle (360° of spindle rotation), the dual drive

motor cylinder block is subjected to the same period of pulsation of each torque as the single emission, for the angular spacing of the adjacent pistons. From Figs. 4, a and b it can be seen that, when the number of internal and external piston emissions is the same, the symmetrical double swashplate structure of the double-sided axial piston motor makes the

torque around the  $x$  and  $y$  axes inside and outside the cylinder block always in opposite directions, so they can cancel each other out to obtain better stability. Without changing other parameters, with an even number of plugs, the cylinder block is subject to lower fluctuations in torque around the  $x$ -axis than with an odd number. However, it is subject to higher than odd fluctuations in moment around the  $y$ -axis. As shown in Fig. 4, c, the output torque produced by the inner and external emissions of the dual drive motor varies in line with that of a normal piston motor. However, the torque generated by the inner and external emissions can be superimposed on each other, which further increases the

power density of the dual drive motor. With an even number of pistons, the magnitude and frequency of fluctuations in internal and external displacement torque superimposed is less than with an odd number of pistons, without changing other parameters. As shown in Fig. 4, d, when the number of pistons in the inner and external emissions is not the same, the total torque generated by the two is superimposed and the total torque fluctuates more irregularly and to a greater extent. In summary, the dual drive motor has the ability to change the torque by varying the internal and external torque parameters, which reduces the amount of overturning torque and torque pulsation.

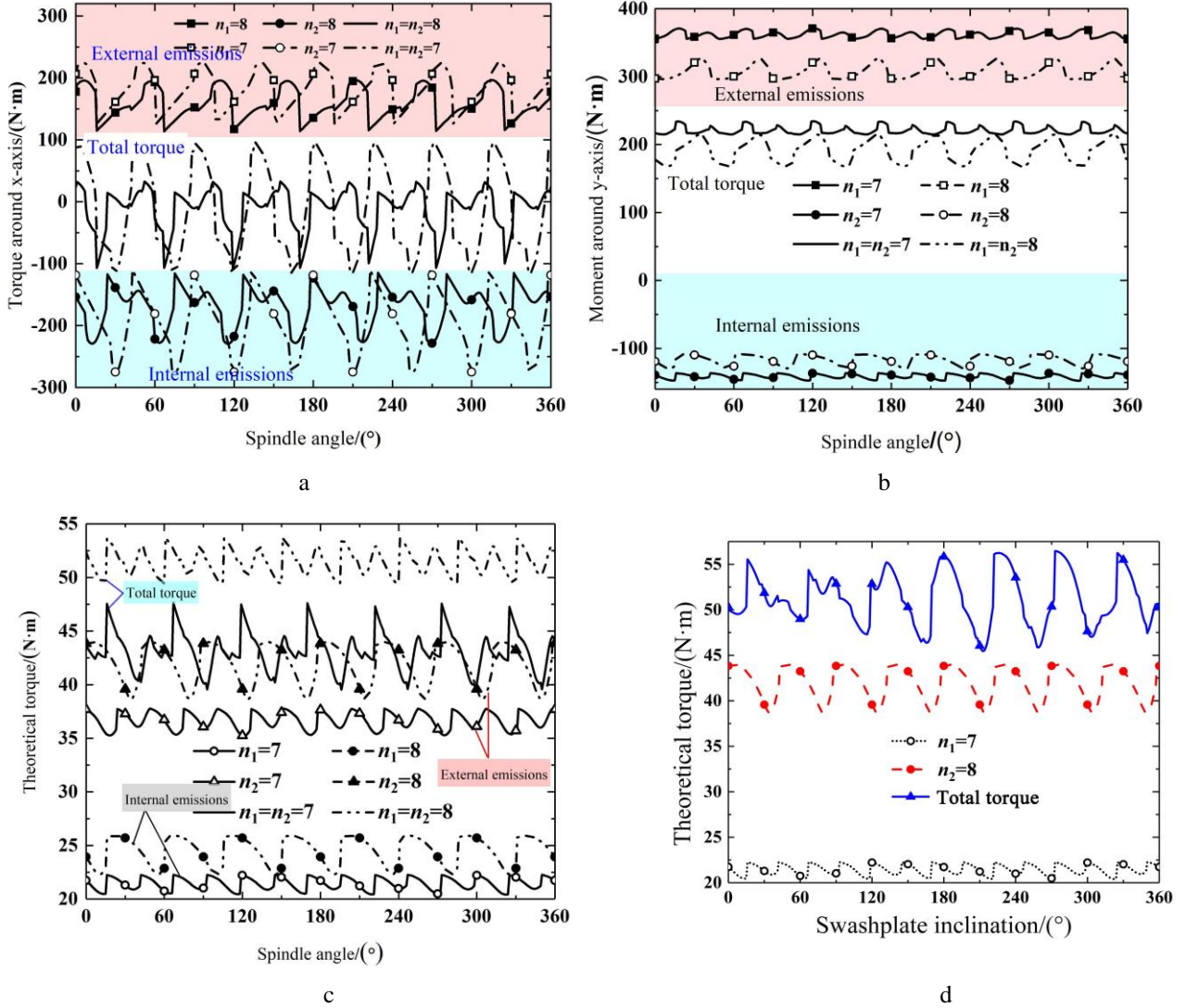


Fig. 4 The effect of the number of plugs on the individual moments of the cylinder block: a - torque around  $x$ -axis; b - moment around  $y$ -axis; c - output torque; d - torque output with different number of internal and external pistons

### 3.2. Effect of staggering angle on cylinder block torque

Fig. 5 shows the effect of staggering angle on the pulsation rate of the cylinder block subjected to torque around each axis and the variation of the magnitude of each torque at different staggering angles. Table 2 shows the peak and valley values of the torque around each axis and the pulsation rate of the cylinder block at different staggering angles. From Fig. 5, a and Table 2, it can be seen that as the staggering angle increases, the pulsation of the cylinder block by the moment around the  $x$ ,  $y$  axis increases first and then decreases, the pulsation rate is the smallest when the

staggering angle is  $0^\circ$ ,  $6.047$  and  $0.072$  respectively. When the staggering angle is  $15^\circ$ , the cylinder block is subjected to the maximum pulsation rate of the moment around the  $x$ -axis. When the staggering angle is  $19^\circ$ , the cylinder block is subjected to the greatest rate of pulsation of torque around the  $y$ -axis. As the staggering angle increases, the output torque of the dual drive axial piston motor first decreases and then increases. Maximum pulsation rate of  $0.104$  at an intersection angle of  $0^\circ$ . The minimum pulsation rate at an intersection angle of  $21^\circ$  is  $0.077$ , a 25% reduction compared to the maximum pulsation rate. The change in stag-

gerring angle does not affect the pulsation period of the respective moments. From Fig. 5, d and the table it is clear that, the peak output torque decreases and the valley increases as the stagger angle corresponding to the maximum pulsation rate changes to the minimum pulsation rate. The change in the staggering angle causes the larger and smaller values of the inner and external emission output torques to be superimposed, reducing the fluctuation and thus the pulsation rate of the torque. And for moments around the x and

y axes, the direction of the torque generated by the inner and external emissions is always opposite. The two can cancel each other out to reduce the overturning moment. And at an intersection angle of 0°, the two fluctuate in almost identical patterns. Larger and smaller values cancel each other out. The fluctuations in torque and the pulsation rate are therefore minimal at this point.

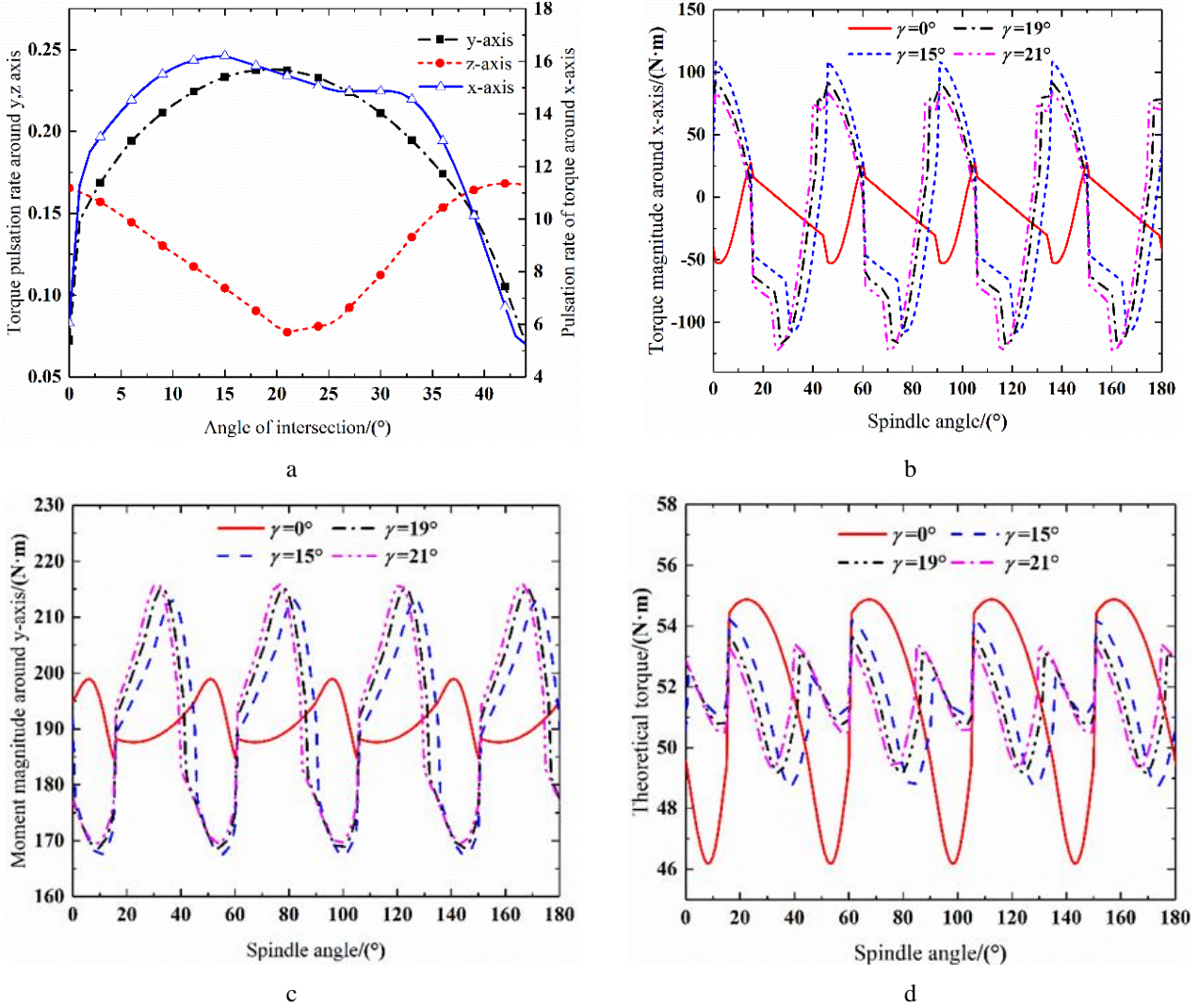


Fig. 5 Effect of staggering angle on each moment of the cylinder block: a - effect of staggering angle on cylinder block torque; b - moment around x-axis at different staggering angles; c - moment around y-axis at different staggering angles; d - output torque at different staggering angles

Table 2

Peak and valley values of torque around each axis and pulsation rate of the cylinder block at different staggering angles

| Angle of intersection, (°) | Torque around x-axis, (°) |              |                 | Moment around y-axis, (°) |              |                 | Output torque, (°) |              |                 |
|----------------------------|---------------------------|--------------|-----------------|---------------------------|--------------|-----------------|--------------------|--------------|-----------------|
|                            | Peak value                | Valley value | Pulsation value | Peak value                | Valley value | Pulsation value | Peak value         | Valley value | Pulsation value |
| 0                          | 27.68                     | -52.87       | 6.047           | 198.96                    | 184.80       | 0.072           | 54.87              | 46.17        | 0.165           |
| 15                         | 108.43                    | -107.59      | 16.214          | 167.42                    | 167.42       | 0.233           | 54.22              | 48.74        | 0.104           |
| 19                         | 91.78                     | -117.46      | 15.710          | 168.60                    | 168.60       | 0.238           | 53.67              | 49.17        | 0.086           |
| 21                         | 83.43                     | -122.42      | 15.451          | 169.52                    | 169.52       | 0.237           | 53.30              | 49.33        | 0.077           |

### 3.3. Effect of oil inlet pressure on cylinder block torque

Figs. 6a to c depict the relationship between each torque and the inlet pressure. Fig. 6, d depicts the magnitude of the pulsation rate of the output torque for different internal and external discharge inlet pressures. Table 3 describes

the magnitude of the fluctuations in the torque around each axis and the pulsation rate of the cylinder block at different inlet pressures. From Fig. 6, a - c and Table 3 it can be found that: When the internal and external oil inlet pressure is the same, as the inlet pressure rises from 22.5 MPa to 31.5 MPa,

the cylinder block is subjected to the torque around x and y axes and the output torque size also increases significantly, the fluctuation of the cylinder block torque around each axis increases, the pulsation rate of the cylinder block torque around x-axis and output torque gradually decreases with the increase of the inlet pressure, while the pulsation rate of the cylinder block torque around y-axis gradually increases with the increase of the inlet pressure. The pulsation rate of the torque around the y-axis gradually increases with the increase of the inlet pressure. Changes in inlet pressure do not affect the individual torque patterns and pulsation periods.

Due to the constructional characteristics of the dual drive motor, the internal and external oil inlets can be independent of each other, and the selection of a suitable inlet pressure can reduce the tipping torque and output torque pulsation rate. As shown in Figs. 6, c and d, the output torque pulsation rate basically increases when the internal inlet pressure remains constant while the external inlet pressure increases. When the external inlet pressure remains constant and the internal inlet pressure increases, the output torque pulsation rate is largely reduced.

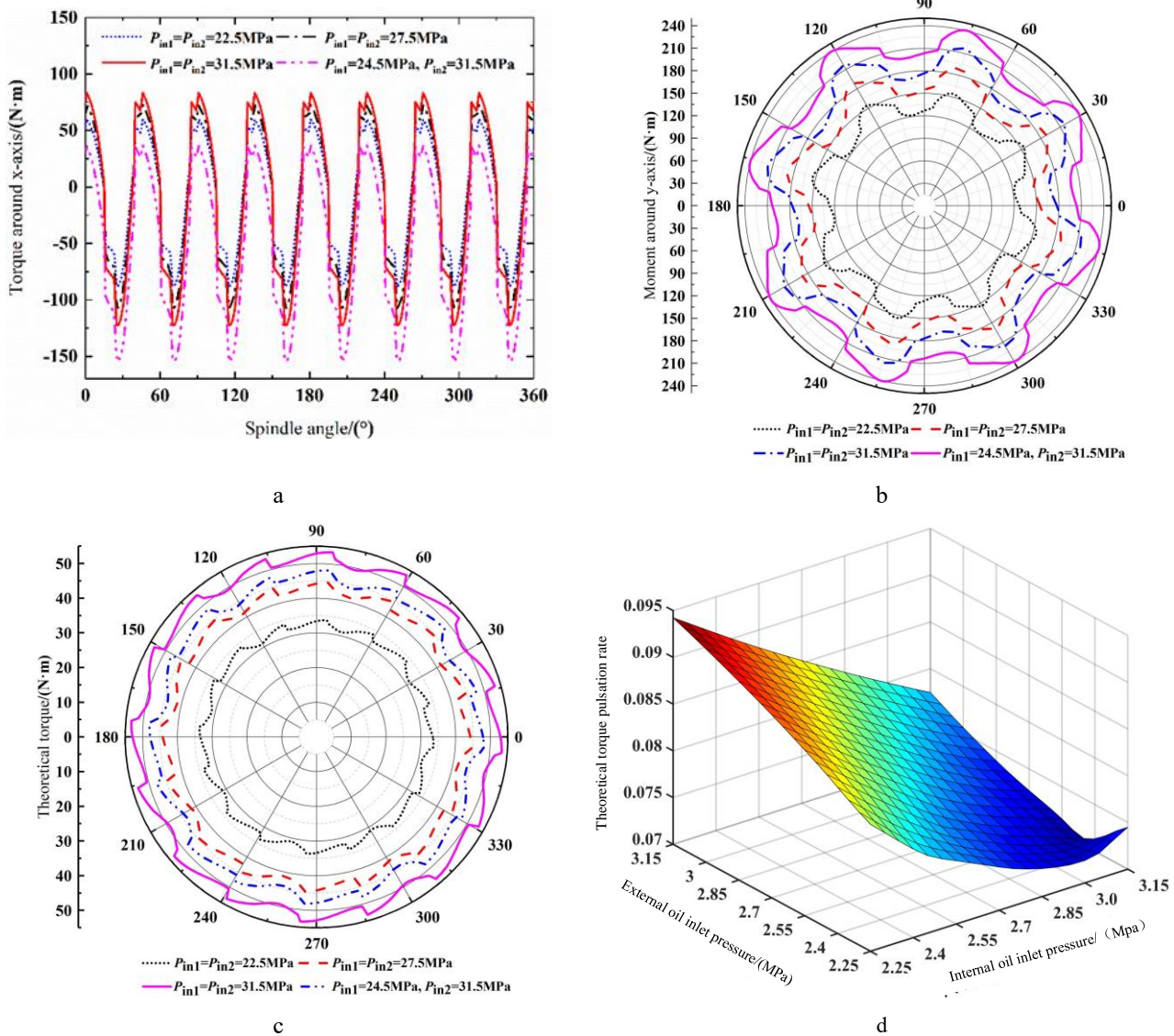


Fig. 6 Effect of oil inlet pressure on each cylinder block torque: a - torque around x-axis; b - torque around y-axis; c - output torque; d - output torque pulsation rate as a function of feed pressure

Table 3

Magnitude of torque fluctuations and pulsation rate of the cylinder block around each axis at different inlet pressures

| Oil inlet pressure     |                   | Torque around x-axis  |                | Torque around y-axis  |                | Output torque         |                |
|------------------------|-------------------|-----------------------|----------------|-----------------------|----------------|-----------------------|----------------|
| Internal emission, MPa | Out emission, MPa | Fluctuation range, () | Pulsation rate | Fluctuation range, () | Pulsation rate | Fluctuation range, () | Pulsation rate |
| 22.5                   | 22.5              | 147.138               | 10.138         | 32.376                | 0.229          | 2.770                 | 0.083          |
| 27.5                   | 27.5              | 179.755               | 9.806          | 40.142                | 0.233          | 3.485                 | 0.079          |
| 31.5                   | 31.5              | 205.857               | 9.481          | 46.433                | 0.235          | 3.978                 | 0.077          |
| 24.5                   | 31.5              | 189.847               | 3.116          | 42.183                | 0.188          | 4.256                 | 0.070          |

3.4. Effect of swashplate inclination on cylinder block torque

Fig. 7, a to c depict the relationship between each moment and the inclination angle of the swashplate. Fig. 7d depicts the magnitude of the pulsation rate of the output torque for different internal and external swashplate inclination angles. From Figs. 7, a - c when the inclination angle of the inner and external emission swashplate is the same, with the increase of the inclination angle, the value of each moment suffered by the cylinder block increases, and the fluctuation amplitude also increases, but the direction of each moment generated by the single inner and external emission does not change with the change of the inclination angle. As the inclination angle of the swashplate can change the magnitude of each torque, and the inner and external swashplate

inclination angles are independent of each other, the appropriate inner and external swashplate inclination angles can be selected to reduce the overturning torque and output torque pulsation rate respectively. From Figs. 7, c and d when the inclination of the inner swashplate is constant and the inclination of the external swashplate increases, the output torque pulsation rate also increases. When the external swashplate tilt angle remains constant and the inner swashplate tilt angle increases, the output torque pulsation rate is reduced. When  $\beta_1 = 16^\circ$  and  $\beta_2 = 11^\circ$ , the output torque pulsation rate is a minimum of 0.0727, when the output torque generated by the inner and external emissions is superimposed with a small fluctuation in the total torque.

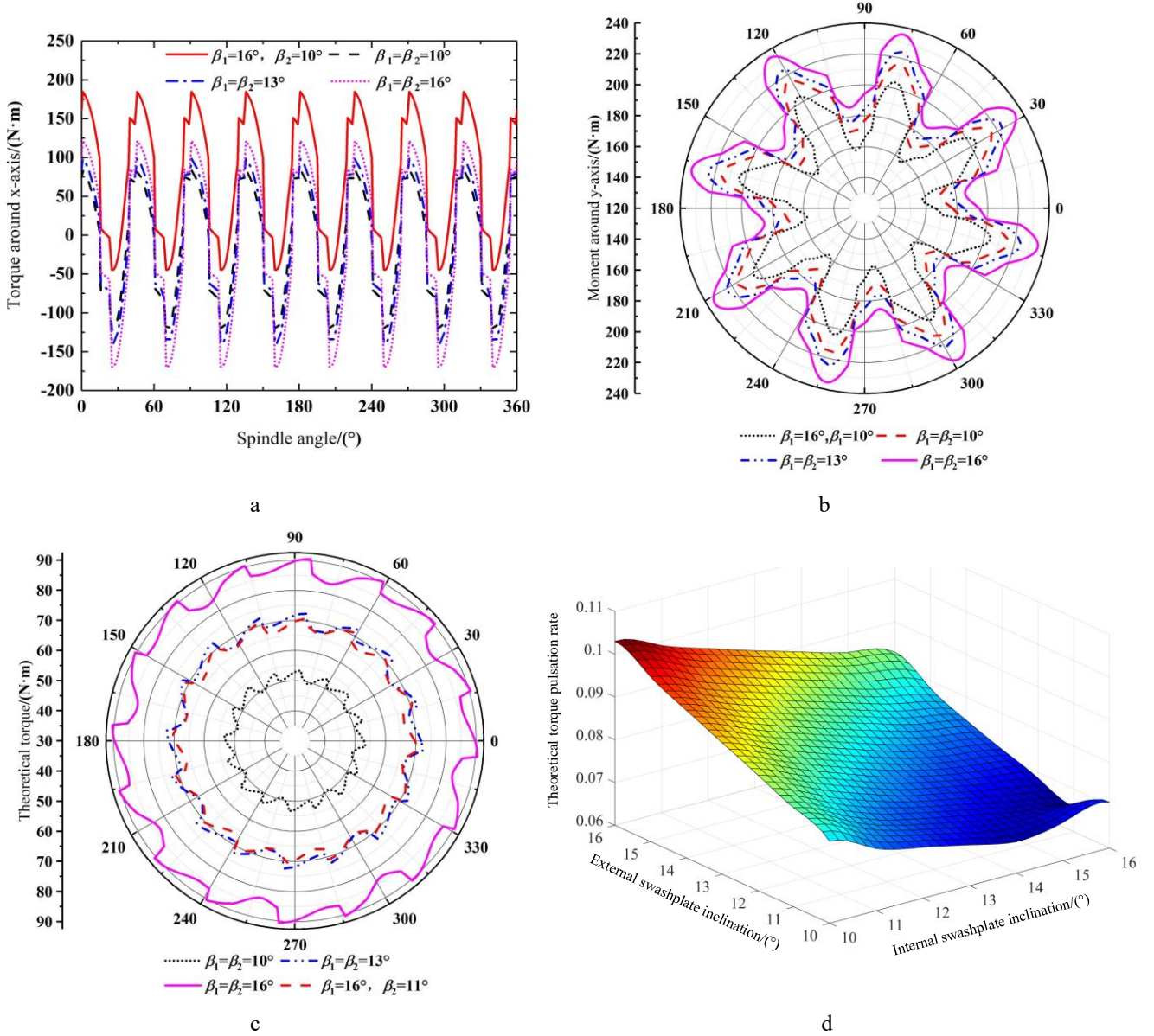


Fig. 7 Effect of swashplate inclination on each cylinder block moment: a - moment around x-axis versus inclination of swashplate; b - moment around y-axis versus inclination of swashplate; c - output torque as a function of swashplate inclination; d - output torque pulsation rate as a function of swashplate inclination

#### 4. Discussion

As seen in Figs. 4 – 7, the number of pistons, staggered angle, inlet pressure and swashplate angle of the inner and external emissions of the axial motor are designed in such a way that the overturning torque and output torque pulsations generated by the inner and external emissions can

be offset. Lower cylinder block tilting torque and lower output torque pulsation than ordinary axial piston motors, resulting in smoother cylinder block movement.

As can be seen in Figs. 4 – 7, the closer the pulsation amplitude of the internal and external displacement torques are and the opposite phase angle, the more effective the

superposition is. However, there is always a certain difference in the torque amplitude of the inner and external emission of torque due to the fact that there is always a certain difference in the size of the distribution circle structure of the inner and external emission of cylinder blocks. This problem can be overcome by coupling the other parameters of the bilaterally driven axial motor to each other. As shown in Fig. 6: The inlet pressure can be increased in equal proportion to the pulsation amplitude. The internal and external torque pulsation can be better counteracted by setting the internal and external discharge pressure ratio inversely proportional to its structural dimensions. The number of internal and external pistons and the inclination of the swashplate can also be combined to optimize the offset effect.

As can be seen from Fig. 5 the staggered angle of the inner and external emission has the opposite effect on the torque pulsation around the  $x$  and  $y$  axes as it does on the output torque. An increase in the internal misalignment angle increases the torque pulsation around the  $x$  and  $y$  axes while the output torque pulsation decreases, both of which conflict with each other. This is because at a staggered angle of  $0^\circ$ , the torques around the  $x$  and  $y$  axes of the inner and external emissions are exactly opposite and cancel out best. And in the same plunger number conditions, at this time the output torque phase angle is the same, can't be offset, can only be directly superimposed and can't reduce the effect of output torque pulsation.

In summary, for dual side drive axial piston motors, the intersection angle should be set as small as possible. Better stability of its cylinder blocks through internal and external displacement pressure ratios and swashplate inclination ratios.

## 5. Conclusion

The paper analyses the forces on the cylinder block of a double-sided driven axial piston motor, a mathematical model of the cylinder block torque was developed and the influence of the number of plugs, staggering angle, Internal pressure and swashplate inclination on the cylinder block torque was analyzed. The following conclusions were reached:

1. When the number of internal and external pistons is the same, the cylinder block is subjected to a cyclic pulsating cycle of each torque in one working cycle. Pulsation period is the angular distance between adjacent pistons. The torque pulsation period of the hydraulic cylinder block is only affected by the number of plugs and the frequency of torque fluctuations is more frequently with odd plugs than with even plugs.

2. As the staggering angle increases, the pulsation rate of the moment around the  $x$  and  $y$  axes tends to increase and then decrease. The output torque varies in the opposite direction. The change in staggering angle does not affect the pulsation period of the respective moments.

3. When the internal and external inlet pressure is the same, the pulsation rate of the cylinder block around the  $x$ -axis torque decreases as the inlet pressure increases. The pulsation rate of the moment around the  $y$ -axis of the cylinder block increases with the increase of the inlet pressure. As the inlet pressure increases, the output torque fluctuation increases, but the pulsation rate decreases slightly. When the internal and external oil inlet pressures are different, the internal and external swashplate tilt angle can be reasonably

changed to increase the output torque while reducing the output torque pulsation rate.

4. When the internal and external oil inlet pressures are different, the internal and external swashplate tilt angle can be reasonably changed to increase the output torque while reducing the output torque pulsation rate. The tilting moment around the  $x$  and  $y$  axes of the cylinder block will increase as the tilt angle increases, and so will the fluctuation. When the internal and external swashplate inclination angle is not the same, the reasonable selection of different internal and external swashplate inclination angle can make the internal and external emissions produce a greater degree of offset of the overturning moment, can reduce the cylinder block overturning moment.

## Acknowledgements

This study was financially supported by the Project (GXXT-2019-048) supported by the University Synergy Innovation Program of Anhui Province and Project (gxbjZD11) supported by the Top-Notch Talent Program of University (Profession) in Anhui Province.

## References

1. **Chao, Q.** 2019. Research on Some Key Technologies of High-speed Rotation for Axial Piston Pumps Used in EHAs [D], Zhejiang university.
2. **Wen, D. S.; Sun, L. J.; Xi, B.,** et al. 2020. Output torque characteristics analysis of double swash plate multi-row axial piston motor, *J. Transactions of the Chinese Society for Agricultural Machinery* v.51(06): 427-433. <http://dx.doi.org/10.6041/j.issn.10001298.2020.06.046>.
3. **Nie, S. L.; Li, Z. Y., Yu, Z. Y.** 2002. Study on torque characteristic of axial piston hydraulic motor, *J. Hydraulics Pneumatics & Seals* (07): 7-10. <http://dx.doi.org/10.3969/j.issn.1000-4858.2002.07.003>.
4. **Xie, J. H.; Liu, J.; Shang, J.,** et al. Analysis and calculation of leakage of swash-plate axial piston pump, *J. Fluid machinery* (2): 55-58 70. <http://dx.doi.org/10.3969/j.issn.1005-0329.2016.02.012>.
5. **Cao, W. B.; Dong, G. J. C.** 2018. Stress and wear leakage analysis of piston in hydraulic axial piston pump, *J. Journal of Gansu Sciences* 30(05): 106-110. <http://dx.doi.org/10.16468/j.cnki.issn1004-0366.2018.05.020>.
6. **Wieczorek, U.; Ivantysynova, M.** 2002. Computer aided optimization of bearing and sealing gaps in hydrostatic machines- the simulation tool Caspar, *J. International Journal of Fluid Power* 3(1): 7-20. <http://dx.doi.org/10.1080/14399776.2002.10781124>.
7. **Hu, X.; Wang, S. P., Han, L.** 2012. Modeling and simulation on pressure distribution of plane port pair in axial piston pump, *J. Hydraulics Pneumatics & Seals* 32(008): 68-71. [http://dx.doi.org/1008-0813\(2012\)08-0068-04](http://dx.doi.org/1008-0813(2012)08-0068-04).
8. **Wang, Z. Q.; Yang, J.; Zhang, H. Y.,** et al. 2016. Flow field character analysis of piston pump valve plate, *J. Hydraulics Pneumatics & Seals* 36(9): 41-44. <http://dx.doi.org/10.3969/j.issn.1008-0813.2016.09.013>.

9. **Li, S. Z.** 2001. Simulation Study on Stability of Hydraulic Torque of Valve Plate on Cylinder Block in Axial Piston Pump [D]; Gansu University of Technology. [http://dx.doi.org/1000-5889\(2001\)03-0041-03](http://dx.doi.org/1000-5889(2001)03-0041-03).
10. **Narvydas, E.; Dundulis, R., Puodžiūnienė, N.** 2020. Rod end stress analysis for hydraulic cylinder of live floor conveying system, *Mechanika* 26(2):108-113. <http://dx.doi.org/10.5755/j01.mech.26.2.24675>.
11. **Wang, B.** 2009. Real time measurement on lubrication characteristic parameters of plane port pair in axial piston pumps, *J. Transactions of the Chinese Society for Agricultural Machinery* 2009(9): 6. <http://dx.doi.org/CNKI:SUN:NYJX.0.2009-09-044>.
12. **Jivantysyn, M. I.** 2001. *Hydrostatic Pumps and Motors: Principle, Design, Performance, Modeling, Analysis, Control and Testing* [D]; New Delhi: Akademia Books International.
13. **Wang, L.; Deng, H. S.; Guo, Y. C., et al.** 2021. Lubrication characteristics of external return spherical hinge pair of axial piston pump or motor under combined action of inclination and offset distance, *J. Journal of Central South University*. <http://dx.doi.org/10.1007/s11771-021-4776-9>.
14. **Deng, H. S.; Huang, K.; Huang, R., et al.** 2016. Swash plate moment property modeling and analysis of balanced two-ring axial piston pump, *J. Chinese Journal of Engineering Design* 23(06): 592-599. <http://dx.doi.org/10.3785/j.issn.1006754X.2016.06.011>.
15. **Mao, F. Y.; He, S. J.; Wang, L., et al.** 2019. Analysis of influence factors of friction torque of port pairs in axial piston pump /motor with dual-driving, *J. Science Technology and Engineering* 019(034): 157-162. [http://dx.doi.org/1671-1815\(2019\)034-0157-06](http://dx.doi.org/1671-1815(2019)034-0157-06).
16. **Ma, J. E., et al.** Study on flow pulsation and valve plate optimization design of axial piston Pump, *J. Zhejiang University*.

H. S. Deng, W. J. Chai, C. Hu

## ANALYSIS OF CYLINDER BLOCK TORQUE CHARACTERISTICS OF DUAL-DRIVE AXIAL PISTON MOTOR

### S u m m a r y

A mathematical model of the cylinder block moment of a dual-drive axial piston motor considering the dynamic pressure in the piston chamber is developed. The influence of the number of plugs, staggering angle, inlet pressure and swashplate inclination on the individual moments applied to the cylinder block was analyzed. The results show: when the number of pistons in the inner and external emissions is the same, the cylinder block is subjected to a periodic pulsation of each moment and odd-numbered pistons have a higher frequency of torque fluctuations than even-numbered pistons. With increasing intersection angle, the pulsation rate of the torque around the x and y axes tends to increase and then decrease but the output torque varies in the opposite direction; The inlet pressure can increase the torque pulsation rate of the cylinder block in equal proportion. When the inclination angle of the inner and external swashplate is not the same, the reasonable selection of different inner and external swashplate inclination angles can make the overturning torque generated by the inner and external emissions offset and increase, so that the overturning torque of the cylinder block is reduced.

**Keywords:** piston motor, cylinder block, torque, pulsation rate, numerical simulation.

Received May 6, 2021

Accepted April 8, 2022



This article is an Open Access article distributed under the terms and conditions of the Creative Commons Attribution 4.0 (CC BY 4.0) License (<http://creativecommons.org/licenses/by/4.0/>).